

48 **Costin D. Untaroiu**
49 Biomedical Engineering and Applied Mechanics (BEAM) Department
50 Virginia Tech University
51 460 Turner Street, Suite 304. Blacksburg, VA 24061
52 Email: costin@vt.edu
53 ORCID ID: 0000-0002-1813-669X
54
55

56 **Abstract**

57 Truck platooning comprises a number of trucks equipped with automated lateral and longitudinal
58 vehicle control technology, which allow them to move in tight formation with short following
59 distances. This study is an initial step toward developing an understanding of the occupant injury
60 risks associated with the multiple sequential impacts between truck platoons and roadside safety
61 barriers; regardless of whether the crash is associated with a malfunction of automated control or
62 human operation. Full-scale crash impacts of a tractor trailer platoon into a concrete bridge
63 guardrail were simulated for a specific Test Level condition according to the Manual for Assessing
64 Safety Hardware (MASH) standards. The model of the bridge barrier was developed based on its
65 drawings and material properties were assigned according to literature data. The impact simulation
66 of the first impact was validated against a full-scale crash test conducted by the Midwest Roadside
67 Safety Facility (MwRSF) based on resulting vehicle kinematics. Then, a higher-fidelity truck cabin
68 model including interior structures was used to evaluate the occupant dynamics and associated
69 safety risks during the impact event. The injury risks of the truck occupants were evaluated using
70 Hybrid-III (HIII) and Thor dummy occupant models representing a 50th percentile male. The
71 occupant risks of injury calculated at body region level or overall showed low injury probabilities
72 for vehicle occupants. The motions of the dummy model and the injury risks results suggested
73 that the 3-point seatbelt system employed in this study provided good protection for vehicle
74 occupants in this impact scenario. Simulations with the Finite Element (FE) models developed in
75 this study could help to understand the effectiveness of roadside safety device improvements and
76 the necessity of platooning constraint modifications before utilization of truck platooning.

77
78 **Keywords:** *Occupant Injury Assessment; Finite Element Modelling; Impact Biomechanics;*
79 *Occupant Protection; Road Safety Hardware*
80

81

82 **1. Introduction**

83 Recently, a new technology called Cooperative Adaptive Cruise Control (CACC) was
84 developed for improving safety of vehicles following at small inter-vehicle spacing using distance
85 measurement among inter-connected vehicles[1]. Truck platooning is a CACC extension to trucks
86 that uses automated lateral and longitudinal vehicle control while moving in tight formation with
87 short following distances. As technology develops and legislation permits, it is expected a gradual
88 decrease of human involvement from current platoons with fully engaged drivers up to driverless
89 platoons [2]. The impacts of CACC platooning have been mostly analyzed on increasing traffic
90 efficiency in terms of road capacity[3], fuel efficiency[4] and traffic flow stability[5]. A few
91 studies have also analyzed the safety of CACC systems in terms of reducing rear-end collisions
92 risks on freeways [6, 7]. However, based on our knowledge, the capacity of existing roadside safety
93 hardware to resist multiple impacts resulting from a malfunction of the automated control system
94 or human operation have not yet been analyzed. In addition, the occupant injury risks associated
95 with such impacts were previously unknown.

96 In this study, a novel method was developed to numerically simulate multiple sequential
97 impacts of tractor trailers into a concrete barrier corresponding to a truck platooning accident. Full
98 scale crash finite element (FE) simulations, employing an existing tractor trailer model and a
99 detailed model of a concrete bridge system, were setup according to the Manual for Assessing
100 Safety Hardware (MASH) standards for a specific Test Level condition. The vehicle stability and
101 barrier damage were evaluated based on these full scale simulations. Then, the injury risks of truck
102 occupants involved in an errant truck platooning crash were evaluated using the Hybrid-III and
103 THOR dummy occupant models and a truck cabin model including the interior structures. In the
104 future, additional roadside barrier systems, such as less costly systems, could be evaluated using
105 the methodology presented in this study.

106 **2. Methods**

107 The overall approach to assess the occupant injury risks during a truck-to-roadside barrier
108 impact is illustrated in Fig 1. The barrier performance and vehicle stability during full tractor
109 trailer-barrier impacts were assessed by FE simulations. A hybrid platooning of five trucks, with
110 occupants (drivers) in the leading truck and the last truck, was simulated [2, 8]. A cabin-only model
111 with interior parts and a seated dummy was developed to assess the occupants' injury risks. This
112 approach reduces the computational costs and avoids numerical instabilities associated with very
113 large models. Detailed information about this method is provided in the next sections.

114

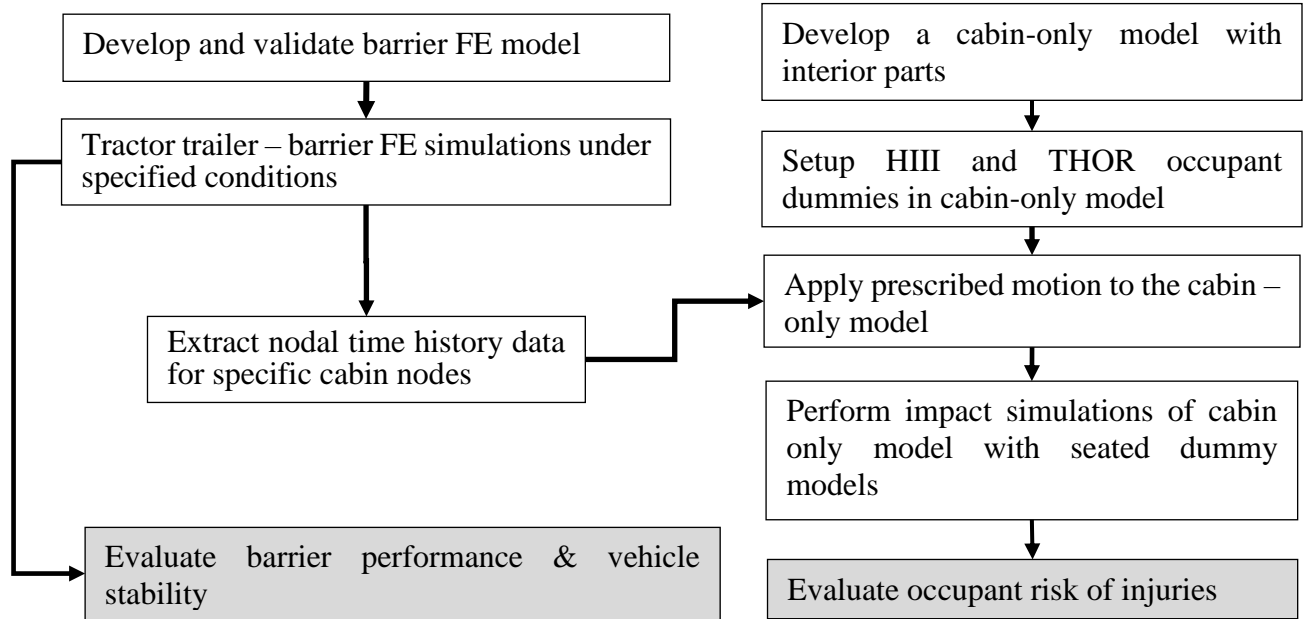


Figure 1. Overall Research Methodology

115
116
117

118 **2.1. Development of the finite element models of the longitudinal barriers**

119 Roadside safety devices are designed to reduce the speed of impacted vehicles and prevent their
 120 impact with fixed objects along the road, reducing the injury risks for vehicle occupants. To
 121 evaluate the vehicle crashworthiness, tractor trailer tests were incorporated from the Manual for
 122 Assessing Safety Hardware (MASH) in Test Level 5 (TL5) and Test Level 6 (TL6) impacts [9].
 123 Flexible systems, such as guardrails, are not designed to preserve their protective capacity after
 124 the first impact. However, other systems such as bridge rails are usually conservatively designed
 125 for the anticipated impact loads, so they may provide some protection to errant truck platoons. As
 126 a first initial step, the impacts to TL5 bridge rails and TL5 median longitudinal barriers were
 127 evaluated in this study. The Manitoba Constrained-Width, Tall Wall Barrier tested at Midwest
 128 Roadside Safety Facility (MwRSF) was selected as a representative bridge rail [10] and the FE
 129 model was developed accordingly.

130 The structure of Manitoba bridge rail consists of a single slope barrier with a height of
 131 1,250 mm (49-1/4 in.), base width of 450 mm (17-3/4 in.) and top width of 250 mm (9-7/8 in.).
 132 The material for the test installation of the bridge rail and deck include concrete mix with 28-day
 133 compressive strength of 45 MPa (6,500 psi) and steel reinforcement consisting of Steel Grade
 134 400W Canadian Metric Rebar [10]. To simulate a joint in the bridge rail and deck, the Manitoba
 135 barrier was designed as two segments – upstream and downstream, with a 168 mm gap between
 136 the segments. Steel end caps were cast into the ends of the bridge rail adjacent to the gap and a
 137 cover plate was placed over the joint and bolted to the upstream side of the barrier. During the
 138 crash testing, the tractor trailer impacted just upstream from the simulated joint in the bridge rail.

139 Transverse rebar spacing in the barrier end section were modified such that the end section had the
140 same capacity as the interior section (i.e. 874 kN -196 kips) to make sure that the interior section
141 of the barrier could also withstand the impact during the crash test [10].

142 The finite element (FE) model of a Manitoba barrier (Figure 2) was developed in LS-Dyna
143 (LSTC, Livermore, CA, USA) based on the drawings of the test installation. The barrier FE model
144 consists of a single segment with total length of 45.72 m (150 ft.), as opposed to the full-scale
145 crash Manitoba barrier testing of the end section in the test MAN-1. Solid brick elements (50 mm
146 x 50 mm) of constant stress were used to model concrete and 2x2 Gauss quadrature beam elements
147 were used to model the rebar in the barrier assembly. MAT_PIECEWISE_
148 LINEAR_PLASTICITY (MAT_024) was selected as the material model for the rebar [11]. The
149 Young's modulus was 200,000 MPa (29,000 ksi), Poisson's ratio was 0.3 and yield strength was
150 400 MPa (58 ksi). A 20% failure strain threshold was specified using element elimination for rebar
151 bars. The constraint of reinforcing steel in concrete was implemented using a
152 CONSTRAINED_BEAM_IN_SOLID (CBIS) card [11]. The concrete elements were modeled
153 using a MAT_CSCM_CONCRETE (MAT_159) [11] with a compressive strength of 45 MPa
154 (6,500 psi). A failure elimination approach defined by a MAT_ADD_EROSION card was used
155 for failure of the concrete model [11]. Effective plastic strain criterion of 9.45% [12] replicated the
156 reasonable concrete erosion observed in the MAN-1 crash test as a result of multiple simulations
157 with various parameters.

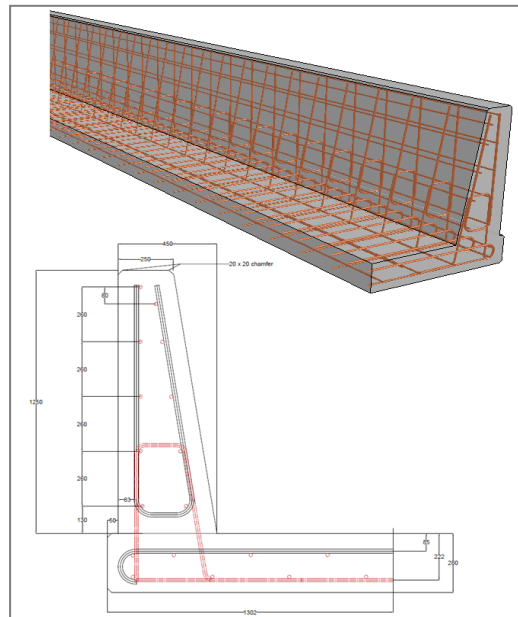


Figure 2: Cross-Section and Layout of Manitoba Barrier FE Model (dimensions in mm)

158

159 **2.2. Simulations of full truck to barriers impacts**

160 To simulate the tractor-barrier impact, an existing Texas Transportation Institute (TTI) proprietary
161 tractor trailer FE model was utilized. This FE model was initially developed by the National Crash
162 Analysis Center (NCAC) [13-15], and then further improved and validated in impact scenarios by
163 TTI. The main TTI improvements included the geometry, mesh size, connections, material
164 properties, and suspension model. The overall length of the trailer was 14.63 m (48 ft.) and the

165 tractor length was 6.5 m (21.2 ft.). The tractor trailer model had 583 parts and 378,901 elements.
166 The weight of ballasted tractor trailer was 36,170 kg (79,741 lbs.).

167 The pre-impact configuration of the tractor trailer model is presented in Figure 3.
168 Appropriate contacts between truck parts and concrete/reinforcement were defined with the
169 friction coefficients between the truck tires and the barrier, the truck body and the barrier, and the
170 truck tires and ground of 0.45, 0.2, and 0.85, respectively [11]. Five impact simulations were
171 performed successively using this configuration. During the simulations, the stresses and
172 displacements of the impacted barrier were recorded in ASCII files called “dynain” [11] and used
173 in the following truck-barrier impact simulations. In a real errant truck platooning accident could
174 be complex and may involve impacts between trucks as well. In this study, the worst safety
175 condition for the barrier was simulated, when it is impacted at the same location by all five trucks
176 in the same pre-impact configuration.

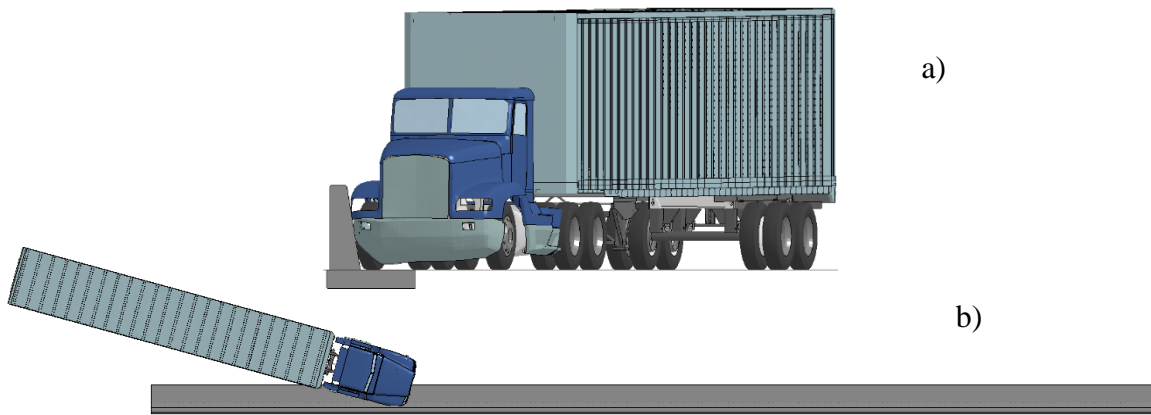


Figure 3: Front (a) and Top View (b) of tractor trailer at the beginning of impact

177

178 **2.3. Development of finite element model of truck cabin used in occupant injury risk** 179 **assessment**

180 The cabin part of the tractor trailer finite element model was extracted and further used to develop
181 the cabin-only model. The interior cabin parts were not included in the original full tractor trailer
182 model, so the seats and the steering column system from another truck FE model were used. The
183 material models of the interior parts were defined based on similar data from publicly available
184 FE vehicle models or in-house material data [16, 17].

185 The motion of the cabin-only model was prescribed using the displacement time histories of 8
186 nodes recorded in the tractor trailer during full scale barrier impact FE simulation. Four of the
187 nodes were located on the cabin floor and the other four nodes are located on the cabin roof (Fig.
188 4a). The selected nodes were selected to be symmetrical about the longitudinal axis of the cabin.
189 To verify the accuracy of the cabin-only model motion, four nodes (other than the nodes used in
190 prescribed motion -Fig. 4b) were selected and their displacement time histories were compared
191 with the same nodes of the full tractor trailer model.

192

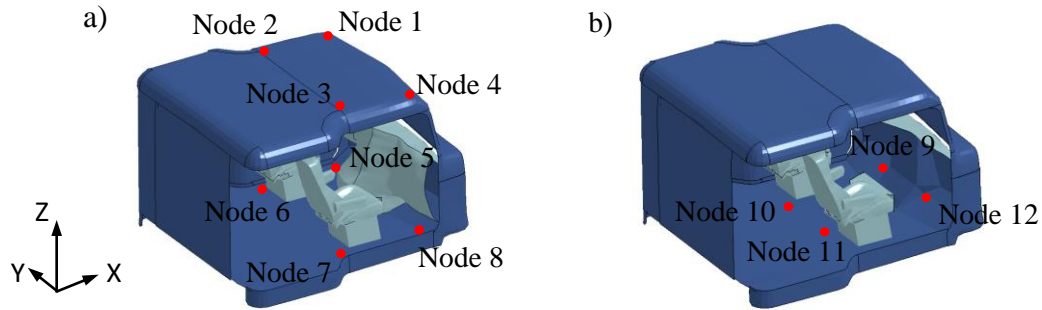


Figure 4. a) The locations of prescribed motion points in the cabin-only model b) The locations of nodes used to verify the cabin motion.

193

194

195 To assess the occupant injury risk, the Hybrid-III and the THOR dummy models [16, 18-
 196 20], the most widely employed frontal automotive dummies, were placed within the cabin-only
 197 model. The FE model of the Hybrid-III dummy used in this study was provided by LSTC
 198 (Livermore, CA, USA)[21]. The Hybrid-III model consists of 367 parts, 276,025 nodes and
 199 451,769 elements, and it was validated at component level against various certification test data
 200 (e.g. neck extension/flexion, thorax impact). The FE model of the THOR (Test device for Human
 201 Occupant Restraint) dummy was developed by NHTSA and their collaborators [22] and updated
 202 according to recent modifications [18, 19]. The THOR FE model consists of 222,292 nodes and
 203 444,324 elements. Similarly, the THOR FE model was validated by CIB-VT computational group
 204 against component certification test data [16, 18, 19].

205 A single occupant dummy model was positioned in the driver’s seat with hands holding
 206 the steering wheel, and feet placed on the floor [23]. The setup for both dummy models used the
 207 same standard three-point belt seatbelt system[24], developed based on LSTC seatbelt model (Fig.
 208 5).

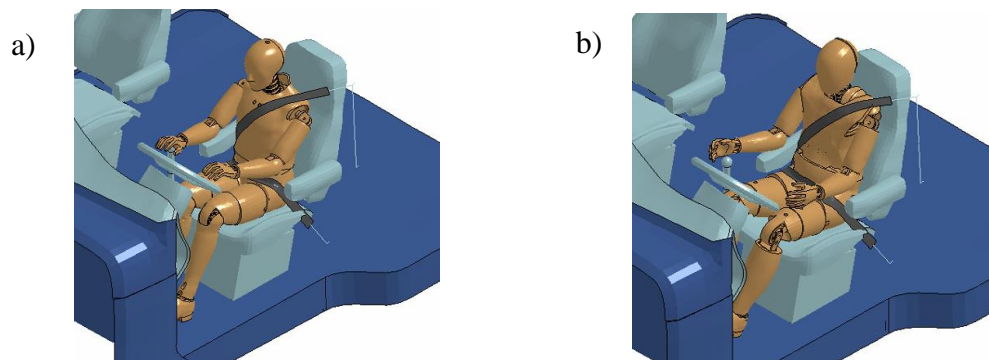


Figure 5. Occupants models seated inside the simplified cabin model a) Hybrid-III dummy model b) THOR dummy model

209

210 Initially, a pretensioner model was fired at the first contact of the truck and barrier model.
 211 However, it was found that the occupant seat lateral (y-direction) acceleration due to offset impact
 212 with the barrier model started to increase after 0.2s (Fig. 6).

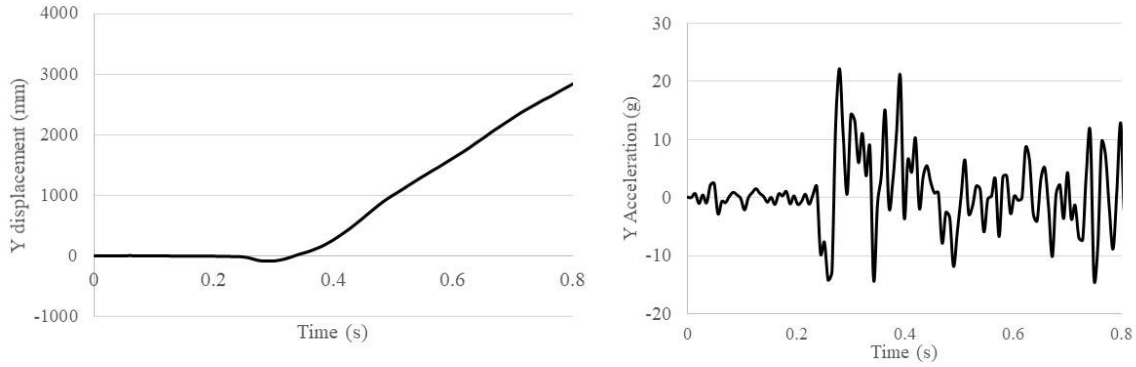


Figure 5. The time histories of displacement (a) and acceleration (b) recorded at the floor node 11.

213
214
215
216
217
218
219
220
221
222

To reduce the computational effort, the beginning of impact (first 0.2 s) was not simulated, so the pretensioner system was not activated. However, the seatbelt system was setup in a configuration close to a post-firing configuration. For example, the seatbelt elements were defined as zero initial slack length with 3 mm minimum length and the webbing fed length in retractor was 10 mm. The friction coefficients in seatbelt - D-rings and dummy-seatbelt contacts were defined as 0.1 and 0.4, respectively. The restraint system included also a frontal-airbag system which was turned off to evaluate the effectiveness of the belt system. It should also be mentioned that airbag systems are not commonly installed in medium/heavy trucks being non-mandatory[25, 26].

223 **2.5. Assessment of truck occupants' injury risks involved in a truck platoon-barrier crash**

224
225
226
227
228
229
230

The kinetic and kinematic responses of dummy FE models recorded during impact simulations were used to calculate injury criteria (Appendix A) to various occupant body regions[27-29]. Then, these measures were compared to the injury assessment reference values (IARVs) and Abbreviated Injury Scale (AIS) to assess the occupant injury risks. The values of the injury assessment reference values (IARVs) represent the borders between acceptable and marginal ratings for a given injury parameter recorded during a crash test (Table 1). Acceptable ratings correspond to measures below the IARVs indicated in the table below.

Table 1 Injury Parameter Cutoff Values Associated with Injury Protection Ratings (50th male)

Body Region	Parameter	IARV
Head	HIC-15	700
Neck	N _{ij}	1.00
	Neck axial tension (kN)	3.3
	Neck compression (kN)	4.0
Chest	Thoracic spine acceleration (3 ms clip,g)	60
	Sternum deflection (mm)	-50
	Sternum deflection rate (m/s)	-8.2
	Viscous criterion (m/s)	1.0
Leg and foot	Femur axial force (kN)	-9.1
	Tibia-femur displacement (mm)	-15
	Tibia index (upper, lower)	1.00
	Tibia axial force (kN)	-8.0
	Foot acceleration (g)	150

231

232 **3. Results and Discussion**

233 **3.1. Barrier Performance**

234 The full scale tractor trailer- barrier simulation was performed corresponding to the MAN-1 test
 235 [10], with the pre-impact tractor speed of 83.2 km/h (51.7 mph) at an angle of 15.2 degrees relative
 236 to the barrier. According to the simulation results, the tractor-trailer struck the barrier
 237 approximately 10.52 m (34.5 ft) from the upstream barrier end and was successfully contained and
 238 redirected by the barrier (Fig. 7). The barrier experienced a maximum dynamic displacement of
 239 50 mm (1.97 in) about 0.72 seconds after the first contact, which was comparable to the value of
 240 52 mm (2 in) recorded in the MAN-1 test[10]. The permanent nodal displacement of the barrier
 241 from the impact was 44 mm (1.73 in).

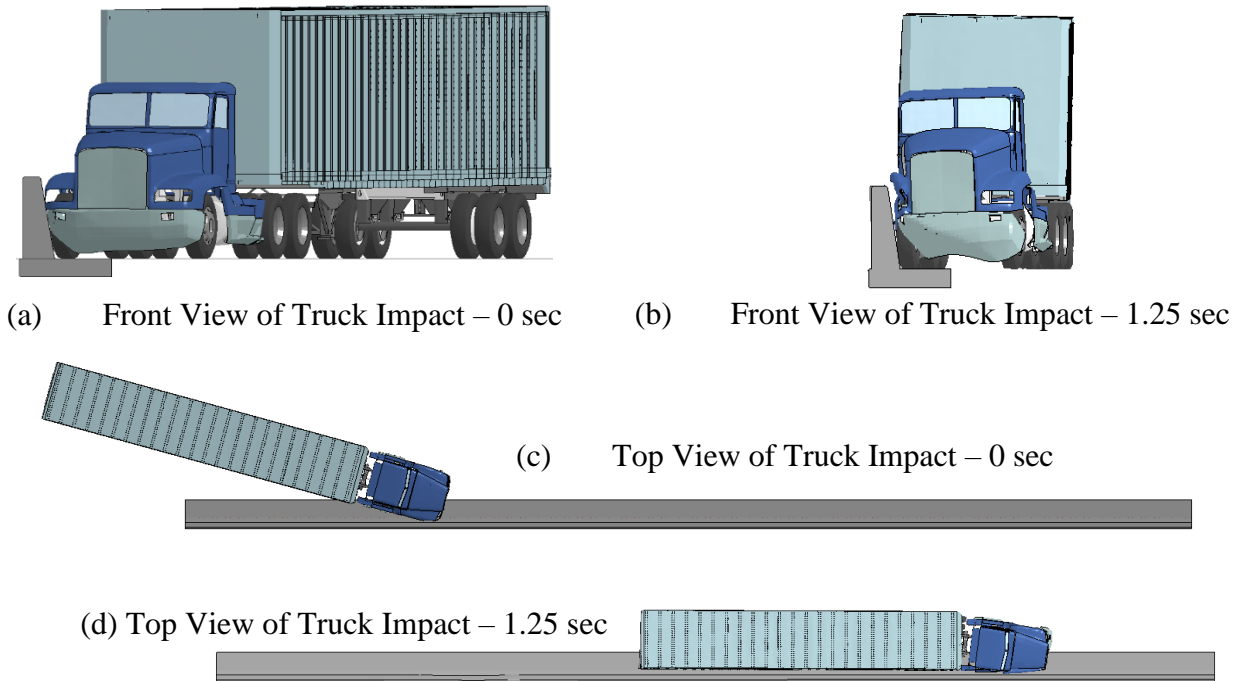


Figure 7: Impact (at 0 sec) and Intermediate (at 1.25 sec) Positions of the Manitoba Barrier

242

243 In terms of barrier damage, erosion at the top of the barrier (Fig. 8) occurred at about 13.19 m
 244 (43.3 ft) from the upstream end and extended about 0.75 m (2.5 ft). Almost all of the 50 mm (2 in)
 245 top layer of solid elements from the front side (impact side) to the back side of the barrier was
 246 eroded at the described location, and a line of second-to-top layer of elements also was eroded on
 247 the front side. At the areas where the concrete strain values were the highest, potential cracks could
 248 be found.

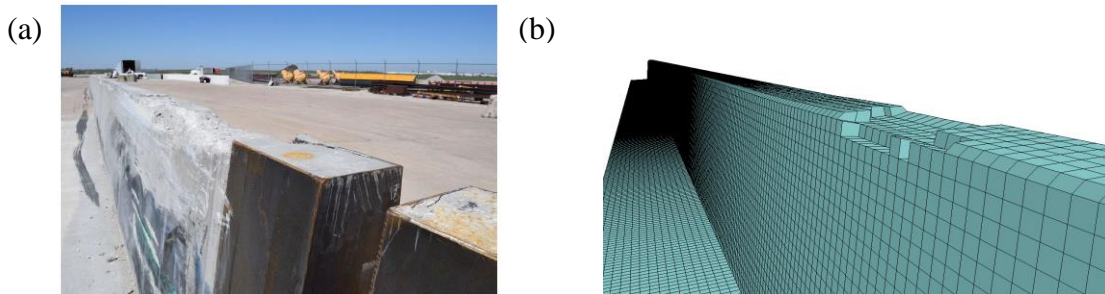


Figure 8: (a) MAN-1 Crash Test – Barrier Damage vs (b) FE Simulation

249

250 The maximum plastic strain of about 5% was observed in transverse rebar in a very small region
 251 at the top of the barrier where the concrete erosion occurred. In addition, most of the reinforcement
 252 had negligible or no plastic strain. Minimal damage occurred on the barrier during the crash test
 253 with contact marks, gouging, spalling and minor cracking. Concrete spalling with maximum depth
 254 of 52 mm (2 in) was observed beginning at the downstream end of the joint cap, i.e. 11.85 m (38.9
 255 ft) from the upstream end of the barrier setup, and extended about 1 m (37 in) downstream [10].

256 The design of the Manibota barrier in this study was shown to be reliable enough to prevent
257 rollover during the impact event, and the stability of vehicle was also guaranteed [30]. The damage
258 to the barrier was small, only about 5% maximum plastic strain, and was observed only in a very
259 small region at the top of the barrier where the concrete erosion occurred. For the most part of the
260 reinforcement, negligible or no plastic strain was observed.

261 **3.2. Vehicle Stability**

262 The physical tractor and the FE tractor model were both stable during the impact events without
263 rollover (Fig. 9 and 10). During the impact simulation (2 sec after initial impact), about 20% of
264 the tractor's initial kinetic energy was dissipated in the form of sliding interface energy. Similarly,
265 the amount of initial kinetic energy converted to internal energy was about 5%. In addition, the
266 hourglass energy of the system was less than 1%.

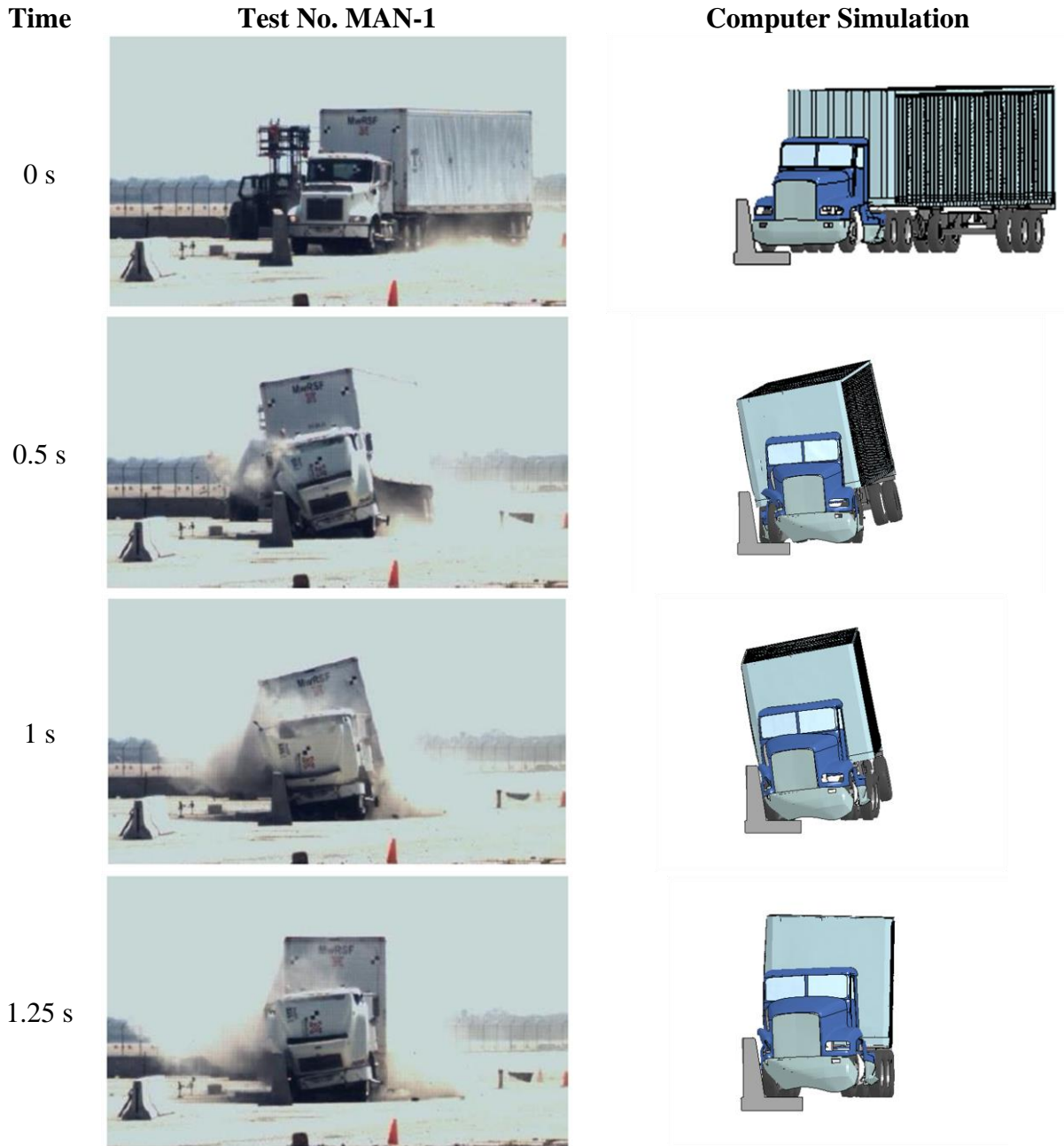


Figure 8: Frame Comparison of Full-Scale Crash Test (MAN-1) and Computer Simulation – Front View (Rosenbaugh et al., 2016)

Figure 9: Frame Comparison of Full-Scale Crash Test (MAN-1) and Computer Simulation – Front View (Rosenbaugh et al., 2016)

267

268

269

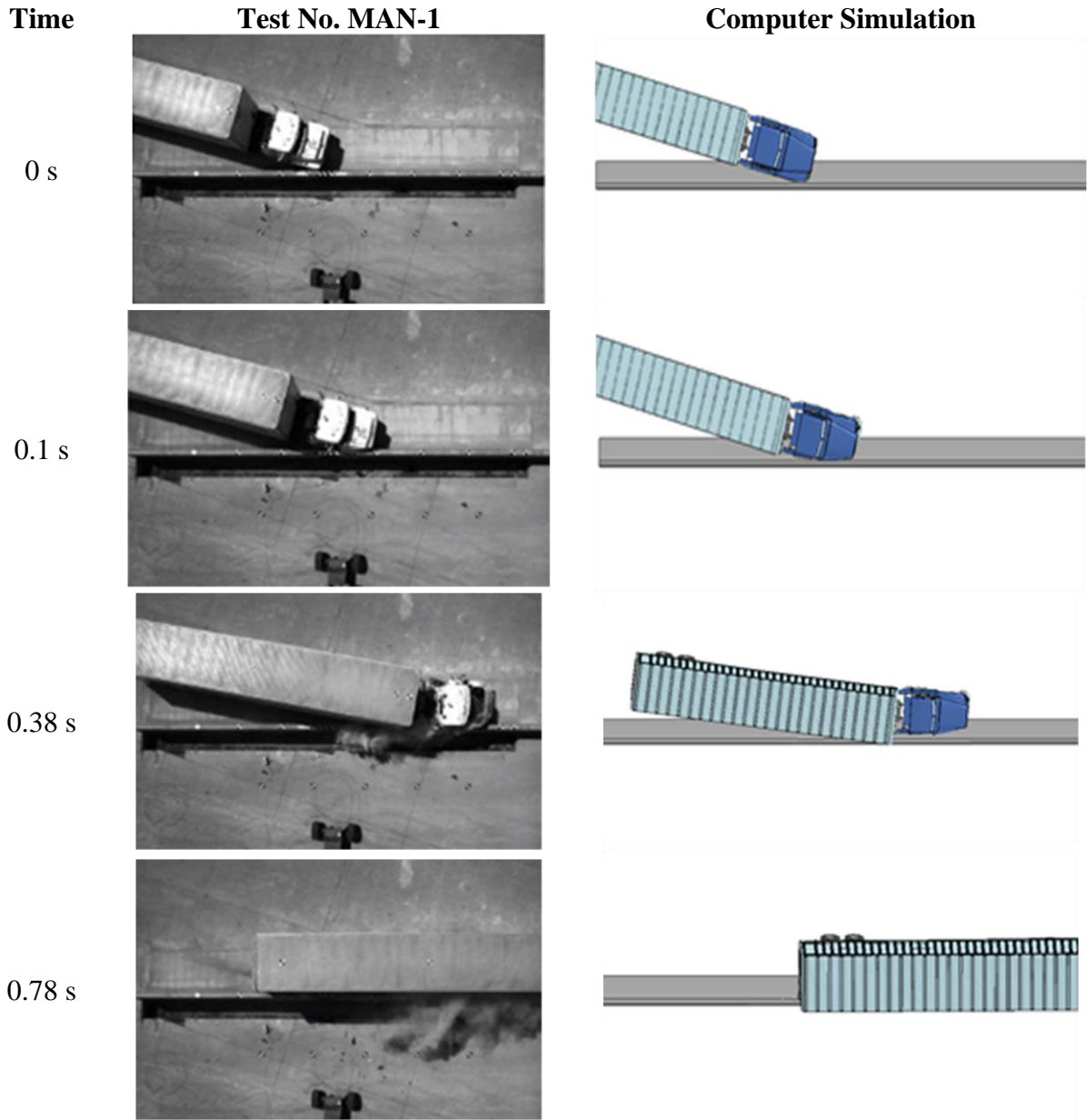


Figure 9: Frame Comparison of Full-Scale Crash Test (MAN-1) and Computer Simulation – Top View (Rosenbaugh et al., 2016)

Figure 10: Frame Comparison of Full-Scale Crash Test (MAN-1) and Computer Simulation – Top View (Rosenbaugh et al., 2016)

270

271

272 **3.3 Assessment of tractor occupants' injury risks involved in a truck platoon-barrier crash**

273 The assessment of tractor occupants' injury risks involved in a truck platoon-barrier crash was
 274 performed using the cabin only model, which included interior parts and dummy models. The
 275 overall kinematics of this cabin-only model showed to be similar to the kinematics of the full
 276 tractor trailer. The displacement differences of the four nodes randomly chosen were very low in
 277 horizontal (x/y) direction (less than 5mm), and slightly higher in vertical (z) direction (under 1.7
 278 cm). Therefore, the cabin only model was then used in the occupant injury assessment. Generally,
 279 in both simulations with HIII and THOR dummies, the seatbelt system was able to effectively
 280 protect the occupant, thus no impacts between the dummy and other interior tractor parts (except
 281 the seat) were observed. (Fig. 11).
 282

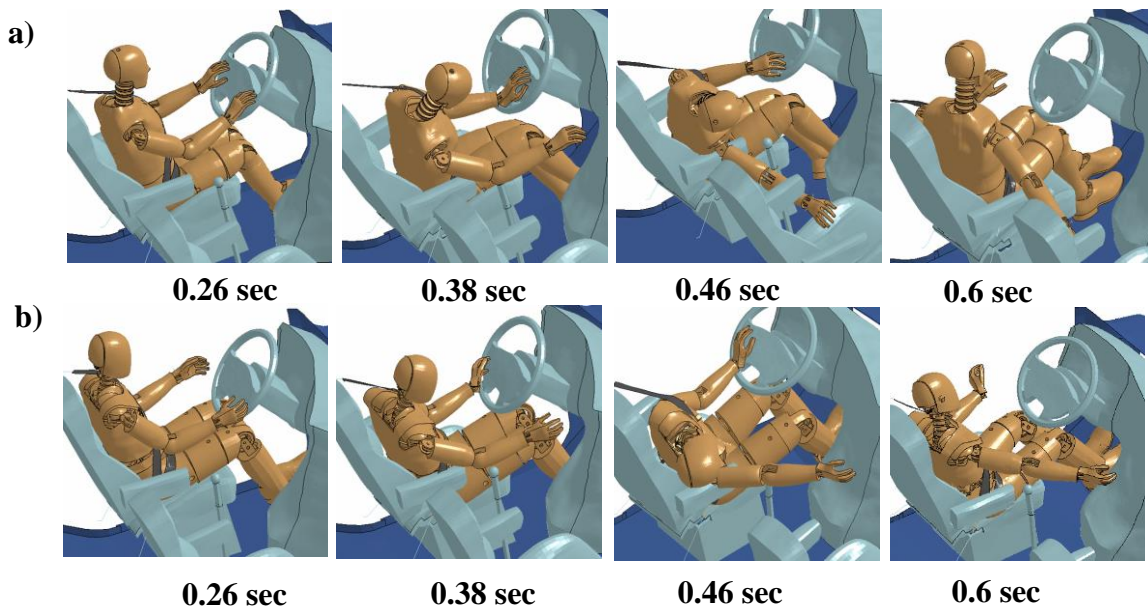


Figure 11. Motions of occupant models during 1st tractor impact, a) Hybrid-III dummy model b) THOR dummy model

283
 284 Although some differences are observed in dummy kinematics between Hybrid-III and THOR
 285 dummy models, possibly caused by different interactions with the seat belt, the predicted values
 286 of injury criteria were close (Table 2). Overall, the impact scenario based on the MAN-1 test
 287 showed to be much less aggressive than a typical front crash scenario, which resulted in a very low
 288 injury risk for truck occupants.

Table 2. The injury risk of tractor drivers predicted by Hybrid III and THOR FE models

Occupant Model	Impact #	Head HIC-15	Neck N _{ij}	Chest Chest Deflection	Femur Femur Axial Force
Hybrid-III (value/injury probability)	1 st	81.2 / 0.00%	0.40 / 8.02%	11.40 mm / 4.03%	845.366 N / 0.90%
	5 th	18.9 / 0.00%	0.23 / 5.87%	7.71 mm / 3.40%	684.85 N / 0.85%
THOR (value/injury probability)	1 st	135.7 / 0.03%	0.47 / 9.10%	28.52 mm / 1.36%	574.18 N / 0.82%
	5 th	124.1 / 0.02%	0.38 / 7.74%	17.28 mm / 0.10%	510.71 N / 0.81%

289
 290 The maximum values of injury criteria recorded during the crash simulation showed to be well
 291 below the IARVs values, which suggested very low injury risk for truck occupants. Three injury
 292 values (HIC, chest deflection, and femur axial forces) were less than 20% of IARVs. The larger
 293 displacement of upper body during the impact event may cause the increased risk of neck injury
 294 compared to other body parts. For the same reason, chest injury probability is the second highest
 295 among all four body regions covered in this study, whereas, it is still relatively low (less than 4%
 296 for two dummies). In addition, the 1st impact and the damage to the barrier from that impact were
 297 reflected in the outcome of the 5th impact for occupant injury risk evaluation. The values of injury
 298 criteria for the drivers of the 5th tractor (the last of the platoon) were lower than the drivers of the
 299 1st tractor caused by a soften pulse generated by the barrier which suffered 5 consecutive impacts.
 300 As long as the barriers are reliable, the occupant injury risks are limited for truck platooning.
 301 The predicted Occupant Injury Measure (OIM) (Appendix A) from both dummy models were
 302 lower than 15%, which corresponds to relatively low injury risks for occupants. The predicted
 303 OIM results from both dummies are also very close (Table 3), which proved the effectiveness of
 304 both dummies to be used in the injury assessment.

Table 3. Occupant Injury Measure

OIM	Value (1 st / 5 th Impact)
Hybrid-III	12.52% / 9.84%
THOR	11.07% / 8.76%

305
 306 While this study is the first attempt to evaluate the occupant safety during truck platooning
 307 impact, it has also several limitations that should be acknowledged. The Manibota barrier model
 308 developed in this study was validated only to the first impact, so validations to sequential impacts
 309 should be performed in the future when test data will be available. More validations of the tractor
 310 model, which should cover the failure of their parts, are recommended. This will allow to evaluate
 311 to what extent the wreckage of the trucks preceding the last truck would present an additional and
 312 possibly more severe hazard to the operator of the last truck. In this study, dummy models were
 313 positioned in a nominal/standard driver pre-impact posture, but various out-of-position pre-crash
 314 occupant postures are expected in future automated trucks. Therefore, to have a better

315 understanding of the injury risks associated with the tractor occupants after veering off the platoon
316 course, more impact simulations should be performed under pre-impact scenarios (e.g. vehicle
317 impact direction/ impact velocity, driver posture) varied in a parametric fashion (e.g. using DOE).
318 Finally, in addition to HIII and THOR ATD models used in this study, human models with
319 different anthropometries, such as Global Human Body Modelling (GHBMC) models [31-34], are
320 recommended to be utilized in future.

321

322 **4. Conclusions**

323 An errant truck platooning impact event was studied using a detailed reinforced barrier and deck
324 model. The performance of the developed barrier FE model was evaluated using the initial impact
325 and then used in successive truck impacts corresponding to a five-truck platoon. From the
326 simulation results, the designed road safety hardware was able to contain and redirect the
327 impacting vehicle without rollover. Hybrid-III and the THOR dummy FE models were utilized to
328 assess the injury risk for truck platooning occupant drivers. To reduce the computation cost, a
329 simplified cabin FE model with interior components was developed and verified with full scale
330 tractor trailer motion data. A 3-point seatbelt restraint system was developed for the cabin-only FE
331 model to protect the occupants. The injury risks of the vehicle drivers during the barrier impact
332 were relatively low, which suggested that regular seatbelt system was able protect the occupants
333 in this kind of impact. The methodology presented in this study could also be applied to simulate
334 various impact scenarios from errant truck platoon accidents.

335

336 **Acknowledgements**

337 This collaborative study was supported by the United States Department of Transportation through
338 the Safety through Disruption (Safe-D) University Transportation Center (UTC).

339

340 **References**

- 341 1. Schmidt, K.W., *Cooperative Adaptive Cruise Control for Vehicle Following During Lane*
342 *Changes*. Ifac Papersonline, 2017. **50**(1): p. 12582-12587.
- 343 2. Bhoopalam, A.K., N. Agatz, and R. Zuidwijk, *Planning of truck platoons: A literature*
344 *review and directions for future research*. Transportation Research Part B-Methodological,
345 2018. **107**: p. 212-228.
- 346 3. Kesting, A., et al., *Adaptive cruise control design for active congestion avoidance*.
347 Transportation Research Part C-Emerging Technologies, 2008. **16**(6): p. 668-683.
- 348 4. Adler, A., D. Miculescu, and S. Karaman, *Optimal Policies for Platooning and Ride*
349 *Sharing in Autonomy-enabled Transportation*, in *Workshop on Algorithmic Foundations*
350 *of Robotics (WAFR)*. 2016.

- 351 5. Kikuchi, S., N. Uno, and M. Tanaka, *Impacts of shorter perception-reaction time of*
352 *adapted cruise controlled vehicles on traffic flow and safety*. Journal of Transportation
353 Engineering-Asce, 2003. **129**(2): p. 146-154.
- 354 6. Li, Y., et al., *Reducing the risk of rear-end collisions with infrastructure-to-vehicle (I2V)*
355 *integration of variable speed limit control and adaptive cruise control system*. Traffic
356 Injury Prevention, 2016. **17**(6): p. 597-603.
- 357 7. Li, Y., et al., *Evaluation of the impacts of cooperative adaptive cruise control on reducing*
358 *rear-end collision risks on freeways*. Accident Analysis and Prevention, 2017. **98**: p. 87-
359 95.
- 360 8. Kilcarr, S. *Driverless trucks: where they'll work, where they won't*. 2016.
- 361 9. American Association of State Highway and Transportation Officials. *Manual for*
362 *Assessing Safety Hardware*. 2016 [cited 2016].
- 363 10. Rosenbaugh, S.K., et al., *Development of the Manitoba Constrained-Width, Tall Wall*
364 *Barrier*. 2016, Midwest Roadside Safety Facility: Lincoln, Nebraska.
- 365 11. Hallquist, J.O., *LS-DYNA Keyword User's Manual*. 2016, Livermore Software Technology
366 Corporation: Livermore, California.
- 367 12. Murray, Y.D., A. Abu-Odeh, and R. Bligh, *Evaluation of LS-Dyna Concrete Material*
368 *Model 159*. 2007.
- 369 13. Polaxico, C., et al., *Enhanced Finite Element Analysis Crash Model of Tractor-Trailers*
370 *(Phase A)*. 2008, National Transportation Research Center, Inc., University Transportation
371 Center: Knoxville, TN.
- 372 14. Polaxico, C., et al., *Enhanced Finite Element Analysis Crash Model of Tractor-Trailers*
373 *(Phase B)*. . 2008, National Transportation Research Center, Inc., University
374 Transportation Center: Knoxville, TN.
- 375 15. National Transportation Research Center Inc., *Finite Element Models for Semitrailer*
376 *Trucks*. National Transportation Research Center, Inc., University Transportation Center:
377 Knoxville, TN.
- 378 16. Putnam, J.B., et al., *Finite Element Model of the THOR-NT Dummy under Vertical Impact*
379 *Loading for Aerospace Injury Prediction: Model Evaluation and Sensitivity Analysis*.
380 Journal of the American Helicopter Society, 2015. **60**(2).

- 381 17. Dobrovolny, C.S., et al., *Implications of truck platoons for roadside and vehicle safety*
382 *hardware*. 2019.
- 383 18. Putnam, J.B., et al., *Development and evaluation of a finite element model of the THOR for*
384 *occupant protection of spaceflight crewmembers*. Accident Analysis & Prevention, 2015.
385 **82**: p. 244-256.
- 386 19. Putnam, J.B., J.T. Somers, and C.D. Untaroiu, *Development, Calibration, and Validation*
387 *of a Head-Neck Complex of THOR Mod Kit Finite Element Model*. Traffic injury
388 prevention, 2014. **15**(8): p. 844-854.
- 389 20. Mohan, P., et al., *LSTC/NCAC Dummy Model Development*, in *11th International Ls-Dyna*
390 *Users Conference*, LSTC, Editor. 2010: Dearborn, MI, USA.
- 391 21. Guha, S., *LSTC_NCAC Hybrid III 50th Dummy Positioning & Post-Processing*. 2014,
392 LSTC: Michigan.
- 393 22. Untaroiu, C., et al., *Evaluation of a finite element of the THOR-NT dummy in frontal crash*
394 *environment*, in *ESV Conference*. 2009: Stuttgart, Germany.
- 395 23. Bose, D., et al., *Influence of pre-collision occupant parameters on injury outcome in a*
396 *frontal collision*. Accident Analysis & Prevention, 2010. **42**(4): p. 1398-1407.
- 397 24. Krishnaswami, V.B., D., *Feasibility of Heavy Truck Occupant Protection Measures 2003*,
398 Michigan Transportation Research Institute
- 399 25. Hu, J. and D. Blower, *Estimation of seatbelt and frontal airbag effectiveness in trucks: U.S.*
400 *and Chinese perspectives*. 2013, UMTRI: Ann Arbor, MI.
- 401 26. Woodrooffe, J. and D. Blower, *Heavy Truck Crashworthiness: Injury Mechanisms and*
402 *Countermeasures to Improve Occupant Safety*. 2015, National Highway Traffic Safety
403 Administration: Washington, D.C.
- 404 27. Dobrovolny, C. and N. Schulz. *Development of a Simplified Finite Element Approach for*
405 *INvestigation of Heavy Truck Occupant Protection in Frontal Impacts and Rollover*
406 *Scenarios*. in *14th International LS-DNA Users Conference*. 2016.
- 407 28. Dobrovolny, C.S., et al., *A Base Study to Investigate Mash Conservativeness of Occupant*
408 *Risk Evaluation*. Proceedings of the Asme International Mechanical Engineering Congress
409 and Exposition, 2016, Vol. 12, 2017.

- 410 29. Dobrovolny, C.S., N. Schulz, and D. Blower, *Finite Element Approach to Identify the*
411 *Potential of Improved Heavy-Truck Crashworthiness and Occupant Protection in Frontal*
412 *Impacts*. Transportation Research Record, 2016(2584): p. 77-87.
- 413 30. Sharma, R., *Finite Element Analysis of Truck Platoon Impact into Roadside Safety Barriers*
414 *(Master's Thesis)*. 2018, Texas A&M University.
- 415 31. Mao, H., et al., *Development of a finite element human head model partially validated with*
416 *thirty five experimental cases*. J Biomech Eng, 2013. **135**(11): p. 111002.
- 417 32. DeWit, J.A. and D.S. Cronin, *Cervical spine segment finite element model for traumatic*
418 *injury prediction*. J Mech Behav Biomed Mater, 2012. **10**: p. 138-50.
- 419 33. Untaroiu, C.D., N. Yue, and J. Shin, *A finite element model of the lower limb for simulating*
420 *automotive impacts*. Ann Biomed Eng, 2013. **41**(3): p. 513-26.
- 421 34. Yue, N. and C.D. Untaroiu, *A numerical investigation on the variation in hip injury*
422 *tolerance with occupant posture during frontal collisions*. Traffic Inj Prev, 2014. **15**(5): p.
423 513-22.
- 424 35. Gennarelli, T.A. and E. Wodzin, *AIS 2005: a contemporary injury scale*. Injury, 2006.
425 **37**(12): p. 1083-91.
- 426 36. Corporation, T., *Advanced adaptive restraint systems*. 2017, National Highway Traffic
427 Safety Administration: Washington, DC.
- 428 37. Yoganandan, N., A.M. Nahum, and J.W. Melvin, *Accidental Injury. Biomechanics and*
429 *Prevention* 3rd Edition ed. 2015: Springer.

430

431 **Appendix A. Injury risk prediction and the calculation of the whole-body injury**
 432 **metric**

433
 434 Abbreviated Injury Scale (AIS), created by the Association for the Advancement of Automotive
 435 Medicine (AAAM), is defined to classify the probability of injury and describe the severity of
 436 individual injuries. AIS also represents the threat to life associated with the injury rather than the
 437 comprehensive assessment of the severity of the injury [35, 36]. While descriptions of the injury
 438 criteria used in this study are briefly introduced, the more detailed treatment is referred to literature
 439 [36, 37].

440 **A.1. Head Injury Criteria (HIC)**

441 The head injury criterion (HIC) is defined on the basis of the head acceleration. In the Hybrid-III
 442 and the THOR dummy FE model, the HIC is recorded by nodal output of acceleration from the
 443 center of gravity of the head. HIC15 value are exported from the simulation results which defined
 444 as follows:

445
$$HIC = \max \left[\left[\frac{\int_{t_1}^{t_2} a(t) dt}{t_2 - t_1} \right]^{2.5} (t_2 - t_1) \right]$$

446 The probability of head injury ($AIS \geq 3$) is given by the formula:

447
$$p(fracture) = N \left(\frac{\ln(HIC) - \mu}{\sigma} \right)$$

448 where μ and σ are the cumulative normal distribution parameters ($\mu=7.45231$ and $\sigma=0.73998$).

449 **A.2. Neck Injury Criteria (N_{ij})**

450 Neck injury criteria are defined on the basis of normalized neck injury criteria. N_{ij} is defined as the
 451 sum of normalized values of loads and moments.

452
$$N_{ij} = \frac{F_z}{F_{int}} + \frac{M_y}{M_{int}}$$

453 F_{int} and M_{int} are critical values of force and moment. For the Hybrid-III model, $F_{int} = 4,500$ N and
 454 $M_{int} = 155$ Nm; for the THOR dummy model, $F_{int} = 4113$ N and $M_{int} = 78$ Nm. The probability of
 455 neck injury ($AIS \geq 3$) is given by the formula

456
$$p(AIS \geq 3) = \frac{1}{1 + e^{3.227 - 1.969N_{ij}}}$$

457

458 **A.3. Injury Criteria - Thoracic**

459 Chest deflection relative to the sternum during impact event is used to calculate chest injury
 460 probability. D_{max} is the maximum value of the dummy deflection (D). In the Hybrid-III dummy
 461 model, the chest deflection is obtained by using a rotary potentiometer; in the THOR dummy

462 model, the chest deflection is achieved by measuring nodal distances for both the left chest and
463 right chest. As a result, different probability formula of chest injury ($AIS \geq 3$) are defined for the
464 two dummies. For the Hybrid-III dummy

$$465 \quad p(AIS \geq 3) = \frac{1}{1 + e^{3.7124 - 0.0475D}}$$

466 And for the THOR dummy

$$467 \quad p(AIS \geq 3) = 1 - \exp\left(-\left[\frac{D}{e^{4.4853 - 0.0113age}}\right]^{5.03896}\right)$$

468 Where the displacement D is in mm.

469 **A.4. Injury Criteria - Femur**

470 The risk of femur injury were defined based on the maximum axial femur loads. The probability
471 of femur injury ($AIS \geq 3$) for both the Hybrid-III and the THOR dummies is given by the formula

$$472 \quad p(AIS \geq 3) = \frac{1}{1 + e^{4.9795 - 0.326F}}$$

473 where F is in kN.

474 **A.5. Occupant Injury Measure (OIM)**

475 Occupant Injury Measure (OIM), proposed in the CAMP-ARS study [36], was used to define the
476 overall injury risk, which was calculated by summarizing the individual AIS3+ Injury risk
477 probabilities of each injury risk value.

$$478 \quad OIM_{AIS3+} = \{1 - [1 - p(HIC15)][1 - p(N_{ij})][1 - p(Chest Deflection)][1 - p(Femur)]\}$$